

Solid-solid phase transformation via internal stress-induced virtual melting: Additional confirmations

Valery I. Levitas^{a)}

Center for Mechanochemistry and Synthesis of New Materials, Department of Mechanical Engineering, Texas Tech University, Lubbock, Texas 79409

Laura B. Smilowitz, Bryan F. Henson, and Blaine W. Asay

Los Alamos National Laboratory, Los Alamos, New Mexico 87545

(Received 12 April 2005; accepted 12 September 2005; published online 1 November 2005)

Recently, we predicted a mechanism of solid-solid phase transformation (PT) via virtual melting at 121 K below the melting temperature. We report additional experimental and theoretical results for PTs among three polymorphs of the energetic material HMX, α , β , and δ that support this mechanism. In particular: (a) the predicted velocity of interface propagation for $\beta \rightarrow \delta$ PT and overall kinetics of $\delta \rightarrow \beta$ PT are in agreement with experiment; (b) the energy of internal stresses is sufficient to reduce the melting temperature from 520 to 400 K for $\delta \rightarrow \beta$ PT; (c) the nanocracking that appears during solidification does not change the PT thermodynamics and kinetics for the first and the second $\beta \leftrightarrow \delta$ PT cycles; (d) $\delta \rightarrow \beta$ PT starts at a very small driving force; (e) $\delta \rightarrow \alpha$ and $\alpha \rightarrow \delta$ PTs do not occur above 400 K and below 461 K, respectively. © 2005 American Institute of Physics. [DOI: 10.1063/1.2126795]

For a solid-solid phase transformation (PT), the transformation strain tensor ϵ^t transforms the unit cell of the parent phase into the unit cell of the product phase. For a PT with a coherent interface and a large ϵ^t , a huge amount of elastic energy due to internal stresses can be accumulated. Elastic energy reduces the driving force for a solid-solid PT. Also, a moving interface is subjected to resistance due to the interaction with the stress field of crystal lattice defects. If the driving force for the PT (including negative contributions due to elastic energy) is smaller than the athermal (long-range) part of the resistance force k , which acts as dry friction, interface propagation will be arrested. The elastic energy can be reduced through such relaxation mechanisms as dislocation generation and motion, twinning, and fracture. Internal stresses and the mechanism of their relaxation significantly affect the thermodynamics and kinetics of the solid-solid PT, as well as the resulting microstructure.

In Ref. 1, we predicted virtual melting (VM) as a mechanism of stress relaxation and loss of coherence at a moving solid-solid interface. If melting occurs along the interface, the elastic energy completely relaxes. This change in elastic energy increases the driving force for melting and reduces the melting temperature. Immediately after melting, stresses relax and the unstable melt phase (m) crystallizes in a stable product phase. The melt in each transforming material point exists during an extremely short time that is nonetheless sufficient for stress relaxation. It is therefore a transitional activated state rather than real (thermodynamically stable) melt. We called this state the virtual melt. Liquid, as the hydrostatic medium, does not interact with the stress field of crystal defects; consequently, $k=0$. Further consideration drives us to the conclusion that fast solidification in a thin layer leads to nanoscale cracking. All of the above processes repeat themselves at each interface increment. Our theoretical predictions are qualitatively and quantitatively confirmed by seven experimental results^{2,3} on the $\beta \rightarrow \delta$ PT in the organic nitramine ocahydro-1,3,5,7-tetranitro-1,3,5,7-

tetrazocine (HMX) energetic crystal. In particular, it was found, both experimentally^{2,3} and theoretically, that the activation energy for growth is equal to the heat of fusion $\Delta h_{\delta \rightarrow m}$. However, in another paper,⁴ experimental data on the β - δ interface velocity are described by an equation with activation energy equal to $0.42\Delta h_{\delta \rightarrow m}$, which is inconsistent with the VM mechanism. In this letter, we report additional experimental data on interface velocity and demonstrate that the entire set of data in Refs. 2–4 is well-described by a kinetic equation with the activation energy equal to $\Delta h_{\delta \rightarrow m}$. Finally, additional confirmations between the prediction of the VM theory and experiments are reported. New experiments have been conducted similar to those in Refs. 2–4: The samples were heated with a heating rate of 0.08 K/s or slower to a chosen PT temperature and then were held at that temperature. No external mechanical load was applied. Details can be found in Ref. 3.

(a) Interface velocity. In our experiments, an optical movie of the β - δ interface motion was recorded under isothermal conditions at three temperatures: 443, 450, and 458 K. The interface velocity v at several PT stages was determined by dividing the small normal interface displacement by the corresponding propagation time (see diamonds in Fig. 1). Other data based on Refs. 3 and 4 are given in Fig. 1 as well. The VM mechanism results in the following kinetic equation:¹

$$v = v_0 \exp\left(-\frac{\Delta h_{\delta \rightarrow m}}{R\theta}\right) \left[\exp\left(-\frac{\Delta g_{\beta \rightarrow \delta}}{R\theta}\right) - 1 \right], \quad (1)$$

where v_0 is the preexponential factor, R is the gas constant, $\Delta g_{\beta \rightarrow \delta} = \Delta h_{\beta \rightarrow \delta}(\theta - \theta_e)/\theta_e$ is the change in molar Gibbs energy, θ and θ_e are the temperature and β - δ phase equilibrium temperature, and h is the enthalpy. Our middle curve 1 in Fig. 1 is based on Eq. (1) with $\Delta h_{\delta \rightarrow m} = 69.9$ kJ/mol, $\Delta h_{\beta \rightarrow \delta} = 9.8$ kJ/mol,² $\theta_e = 432$ K,⁵ and $v_0 = 10^{10}$ $\mu\text{m/s}$. It is clearly seen from Fig. 1 that the temperature dependence of all experimental data is in agreement with the VM hypothesis. The scatter in data can be described by the scatter in v_0 without changing the temperature dependence. The lower v

^{a)}Electronic mail: valery.levitas@ttu.edu

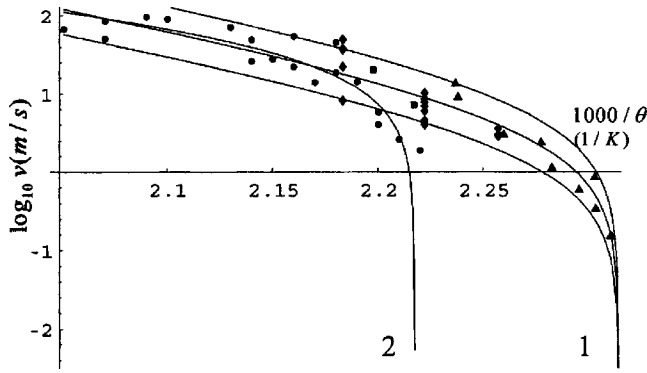


FIG. 1. The logarithm of the interface velocity ($\log_{10}v$) is plotted vs the inverse temperature ($1000/\theta$). Data based on our direct measurements of the propagation of the interface using optical movies of the visible opacity change are plotted as diamonds; data from similar measurements from Ref. 4 are plotted as rectangles; data obtained from the equation $v=l/t_{0.5}$, where $t_{0.5}$ is the half-transformation time from Refs. 2 and 3, and l is the effective propagation length (the same for all points and chosen to yield the best fit) are plotted as triangles. A change in l shifts all triangles in the vertical direction by the same value. Experimental data from Ref. 4 obtained using differential scanning calorimetry measurements are plotted as circles. Lines 1 are based on our Eq. (1) with three different preexponential factors, $v_0=10^{10}$ $\mu\text{m/s}$ for the middle curve; a change in preexponential multiplier by a factor of 2.1 shifts the middle curve by 0.32 up and down. Line 2 is a fit suggested in Ref. 4.

for the three experiments reported in Ref. 4 (Fig. 1) can be explained by difficulties in separation of nucleation and growth in calorimetry tests at low temperature, because direct measurements of v in Ref. 4 (squares in Fig. 1) give much higher values. The curve from Ref. 4 is in qualitative disagreement with experiments below 451 K. The main reason for the lower activation energy in Ref. 4 is the wrong choice of $\theta_e=451$ K while PT proceeds even at 432.6.^{2,3}

(b) Thermodynamic possibility of the VM during the reverse $\delta\rightarrow\beta$ PT. The thermodynamic possibility of the VM mechanism in the $\beta\rightarrow\delta$ PT was proven in Ref. 1. Here we will estimate whether VM can occur during the reverse $\delta\rightarrow\beta$ PT (and if yes, then above what temperature) using the same approach as in Ref. 1. We consider the following transformation process $\delta\rightarrow\beta_{\text{stressed}}\rightarrow\text{VM}\rightarrow\beta_{\text{relaxed}}$ and we need to estimate whether melting of the stressed β phase can occur below 432 K. We will use the equation

$$\theta_m^e = [\Delta h_{\beta\rightarrow m}(\theta_m^e) - g^e] / \Delta s_{\beta\rightarrow m}(\theta_m^e), \quad (2)$$

similar to the one derived in Ref. 1. Here θ_m^e is the melting temperature of the elastically stressed phase, g^e is the energy of internal stresses, and s is the molar entropy. For the reverse $\delta\rightarrow\beta$ PT, the transformation strain tensor $\boldsymbol{\epsilon}_{\delta\rightarrow\beta}^t = -\boldsymbol{\epsilon}_{\beta\rightarrow\delta}^t$ and elastic energy of internal stresses g^e is the same for the $\beta\rightarrow\delta$ PT and the $\delta\rightarrow\beta$ PT; it was estimated as $g^e=9.072$ kJ/mol.¹ We will now show that such an elastic energy can cause the VM of the β phase down to the temperature 400–412 K.

Taking data from Ref. 6 for β phase at $\theta=400$ K ($h_\beta=78.767$ kJ/mol and $s_\beta=387.543$ J/mol K) and extrapolating data from Ref. 6 for melt to 400 K ($h_m=152.743$ kJ/mol and $s_m=544.786$ J/mol K), we obtain from Eq. (2) that the melting temperature of the stressed β phase is $\theta_m^e=412.8$ K. However, if for the case without internal stresses ($g^e=0$) we substitute in Eq. (2) interpolated (for β phase) and extrapolated (for melt) data from Ref. 6 at $\theta=520$ K (melting temperature of the β phase⁵) then we ob-

tain $\theta_m^e=531.3$ K. If we will take into account that the data from Ref. 6 overestimate the melting temperature by ~ 10 K, we may conclude that the the virtual melting of the stressed β phase can occur above 400–413 K. Indeed, there is a small jump to faster transformation rates in the kinetic data (see Fig. 5 in Ref. 3) between two experiments as temperature is reduced from 417 to 394 K, which may serve as an indication of the change in the growth mechanism. Below 400 K, traditional mechanisms of stress relaxation at the moving interface, probably through cracking, have to occur.

Note that if high temperature is reached during or after the $\beta\rightarrow\delta$ PT, chemical decomposition may occur. This may reduce the melting temperature and may broaden the temperature interval in which the VM occurs during the $\delta\rightarrow\beta$ PT.

(c) Overall kinetics of $\delta\rightarrow\beta$ PT. The equation for the rate of the volume fraction of the δ phase, c , has the form $\dot{c}=bv c(1-c)$, where b is a parameter, and $c(1-c)$ is approximately proportional to the total interface area. In Ref. 1, the coincidence of the predicted² overall kinetics for the $\beta\rightarrow\delta$ PT and that experimentally observed in Ref. 3 was proved. However, our equation for \dot{c} is valid for the reverse PT as well, for the driving force $-\Delta g_{\beta\rightarrow\delta}<0$. It coincides with Eq. (13) in Ref. 2 for the growth stage which was also used for both direct and reverse PTs. Our activation energies, $E_{\beta\rightarrow\delta}=\Delta g_{\beta\rightarrow m}$ and $E_{\delta\rightarrow\beta}=\Delta g_{\delta\rightarrow m}$,¹ coincide with activation energies postulated and experimentally confirmed in Ref. 2. The temperature dependence of the rate constant is determined by the heat of fusion $h_{\delta\rightarrow m}$, as in experiments and in Eq. (13) in Ref. 2. Thus, the overall kinetics based on the VM mechanism corresponds to experiments for the $\delta\rightarrow\beta$ PT as well. Note that equation for \dot{c} for the $\delta\rightarrow\beta$ PT can be used above 400–412 K only. At lower temperatures, VM cannot occur and alternative kinetics has to be developed.

(d) Small (negligible) elastic energy and athermal interface friction for $\delta\rightarrow\beta$ PT. For all solid-solid PTs with large transformation strain, the PT start temperature significantly deviates from the θ_e . This occurs mainly due to the elastic energy and athermal interface friction k , according to PT criterion $-\Delta g=k+g^e$. In our experiments,^{2,3} the $\delta\rightarrow\beta$ PT was observed experimentally at 424 K, very close to the $\delta-\beta$ phase equilibrium temperature. We believe that it would be observed at higher temperature as well. However, even such a small overcooling implies small $k+g^e\approx\Delta h_{\beta\rightarrow\delta}(\theta_e-424)/\theta_e=0.181$ kJ/mol. This is negligible in comparison with estimated value of $g^e=9.072$ kJ/mol for this PT without VM,¹ as well as with values $k+g^e$ for all other PTs considered below and in Ref. 1. The only explanation that we see is that $\delta\rightarrow\beta$ PT occurs via VM, which removes k and g^e . Note that the negligible value of $k+g^e$ for the $\beta\rightarrow\delta$ PT was demonstrated in Ref. 1.

(e) Overheating for $\alpha\rightarrow\delta$ PT. The $\alpha\rightarrow\delta$ PT starts at the temperature of 461 K (Ref. 7), which is significantly higher than the $\alpha-\delta$ phase equilibrium temperature of 435 K.⁵ Since the volumetric transformation strain for $\alpha\rightarrow\delta$ PT, 0.046,⁷ is almost two times smaller than that for the $\beta\rightarrow\delta$ PT, g^e is four times smaller, which again favors the $\alpha\rightarrow\delta$ PT. The magnitude of k is proportional to volumetric transformation strain.⁸ This contradiction can be easily explained by the absence of the VM for $\alpha\rightarrow\delta$ PT, because the elastic energy is too small to lower the melt temperature sufficiently. To estimate the driving force for $\alpha\rightarrow\delta$ PT at 461 K, which is

equal to $k+g^e$, we use $-\Delta g_{\alpha\rightarrow\delta}=\Delta h_{\alpha\rightarrow\delta}(461-435)/435=0.40$ kJ/mol, where $\Delta h_{\alpha\rightarrow\delta}=6.7$ kJ/mol.⁷

(f) Absence of $\delta\rightarrow\alpha$ PT above 400 K. Note that in the temperature range $382.4<\theta<435$, the orthorhombic α phase is stable, i.e., $\delta\rightarrow\alpha$ PT rather than $\delta\rightarrow\beta$ PT should occur. Since the volumetric transformation strain for $\delta\rightarrow\alpha$ PT is two times smaller than that for the $\delta\rightarrow\beta$ PT, g^e and k are four and two times smaller, respectively, which has to favor the $\delta\rightarrow\alpha$ PT. However, the $\delta\rightarrow\beta$ PT is the only transition observed in the temperature range $435\text{ K}>\theta>400\text{ K}$.^{2,3} This can again be explained by the fact that the VM mechanism is possible from the β phase while the VM of the α phase is impossible, because its elastic energy and resulting decrease in melting temperature is four times smaller. To estimate the driving force for $\delta\rightarrow\alpha$ PT at 394 K (at this temperature $\delta\rightarrow\alpha$ PT still has not been observed in Refs. 2 and 3 simultaneously with $\delta\rightarrow\beta$ PT), which is equal to $k+g^e$, we use $-\Delta g_{\delta\rightarrow\alpha}=\Delta h_{\delta\rightarrow\alpha}(394-435)/435=0.631$ kJ/mol, where $\Delta h_{\delta\rightarrow\alpha}=-6.7$ kJ/mol.⁷

Note that the values obtained for $-\Delta g_{\delta\rightarrow\alpha}$ may be lower than the actual values of $k+g^e$, because $\delta\leftrightarrow\alpha$ PTs may be facilitated by the stress field of β crystals. Results in (e) and (f) show that without VM, the driving force for the $\beta\leftrightarrow\delta$ PTs has to be higher by a factor of 2–4 than the obtained values for $\delta\leftrightarrow\alpha$ PTs.

(g) Nanocracking and repeatability of the PT kinetics during the cyclic $\beta\leftrightarrow\delta$ PT. Fast solidification in a thin layer created by a moving interface during small time increment has to lead to nanoscale cracking, due to large volumetric contraction. Indeed, considerable cracking, homogeneously distributed in the transformed δ phase over a length scale of several hundred nanometers, accompanies the $\beta\rightarrow\delta$ PT,³ as predicted by theory.¹ However, without VM, stresses during $\beta\rightarrow\delta$ PT in the transformed layer are compressive, since transformation volumetric strain is tensile. Compressive stresses cannot cause the nanocracking. This experimental evidence strongly supports the VM mechanism.

For the reverse $\delta\rightarrow\beta$ PT, during the VM of the stressed β phase, all nanocracks, crossed by the moving interface, disappear, deleting the entire thermomechanical prehistory. During solidification of the melt to the unstressed β phase, new nanocracking has to occur. There are currently no experimental data to check this prediction of our theory. The β phase obtained after PT reversal is indeed cracked but we do not have a proof that these are new nanocracks after the VM of stressed β phase.

In our experiments on PBX 9501 (a formulation of HMX crystals within the polymer binder),^{2,3} the kinetics of the second $\beta\leftrightarrow\delta$ cycle matched well the kinetics of the first $\beta\leftrightarrow\delta$ cycle. The temperatures for the direct and for the reverse PTs were 438 K and 394 K, respectively. Now let us compare two scenarios of the second $\beta\rightarrow\delta$ PT, when the $\beta\rightarrow\delta$ PT occurs without and with the VM. If there is no VM, nanocracks (in fact, it is not clear how nanocracks distributed over the whole transforming volume appear without the VM) generated during the the first $\beta\leftrightarrow\delta$ PT, as well as during the second $\beta\rightarrow\delta$ PT, affect the growth stage.⁸ First, the stress field of the cracks creates an athermal resistance to interface propagation k , just as do other defects. Since the first $\beta\leftrightarrow\delta$ PT generates significant nanocracking, the magnitude of k for the second $\beta\rightarrow\delta$ PT would be much higher. It would shift the kinetic curve to higher temperatures. Second,

new cracks will be generated during the second $\beta\rightarrow\delta$ PT, which will affect the thermodynamics and kinetics of the PT through changes in the stress field.⁷

If the first and second $\beta\rightarrow\delta$ PTs occur via the VM, then $k=0$; and since the new nanocracks are generated during the solidification (i.e., at negligible resistance to the crack appearance), the stress field after the appearance of new nanocracks is zero, the same as before their appearance. This is similar to the first $\beta\rightarrow\delta$ PT. Thus there is no reason why the second $\beta\rightarrow\delta$ PT will differ from the first one, which corresponds to the experiment.^{2,3}

Also, all cracks and other defects that appear during the first $\beta\rightarrow\delta$ PT disappear due to melting and new nanocracks appear during the solidification. Thus, there is no crack accumulation over the PT cycles; the VM deletes the entire thermomechanical memory about the previous $\beta\leftrightarrow\delta$ cycles. That is why the second reverse $\delta\rightarrow\beta$ PT does not differ from the first one, which also corresponds to the experiment.^{2,3} Thus the repeatability of the PT kinetics during the cyclic $\beta\leftrightarrow\delta$ PT, observed experimentally in Refs. 2 and 3, is a very strong argument supporting the VM mechanism of the $\beta\rightarrow\delta$ PT.

Summarizing, there are 14 (seven in Ref. 1 and seven here) theoretical predictions based on the VM mechanisms that are in qualitative and quantitative agreement with experiments conducted on the α , β , and δ PTs in the energetic crystals HMX. None of these results separately proves strictly the validity of the VM. However, because it is difficult to imagine any other mechanism that explains all the above 14 experimental results, we conclude that $\beta\leftrightarrow\delta$ PTs in the HMX crystal occur via VM. Thus, we have found an unexpected mechanism of solid-solid PT, loss of interface coherency, and stress relaxation via VM, much below the melting temperature. The mechanism significantly changes thermodynamics (increases the net driving force and eliminates k) and kinetics (activation energy and rate constant) of solid-solid PT and leads to nanocracking. The VM deletes the entire thermomechanical memory about preceding PT cycles. Note that the VM mechanism simplifies significantly the thermodynamic and kinetic models for large-scale simulation of $\beta\leftrightarrow\delta$ PTs in HMX that are currently under development. The VM can also explain high pressure amorphization in a number of material systems.⁹

V.I.L. acknowledges the support of the NSF (Grant No. CMS-02011108) and LANL (Grant No. 13720-001-05-AH).

¹V. I. Levitas, B. F. Henson, L. B. Smilowitz, and B. W. Asay, *Phys. Rev. Lett.* **92**, 235702 (2004).

²B. F. Henson, L. B. Smilowitz, B. W. Asay, and P. M. Dickson, *J. Chem. Phys.* **117**, 3780 (2002).

³L. B. Smilowitz, B. F. Henson, B. W. Asay, and P. M. Dickson, *J. Chem. Phys.* **117**, 3789 (2002).

⁴A. K. Burnham, R. K. Weese, and B. L. Weeks, *J. Phys. Chem. B* **108**, 19432 (2004).

⁵H. H. Cady and L. C. Smith, *Studies on the Polymorphs of the HMX*, Report No. LAMS-2652, 1962 (unpublished).

⁶J. L. Lyman, Y. C. Liau, and H. V. Brand, *Combust. Flame* **130**, 185 (2002).

⁷M. Herrmann, W. Engel, and N. Eisenreich, *Propellants, Explos., Pyrotech.* **17**, 190 (1992).

⁸V. I. Levitas, *Continuum Mechanical Fundamentals of Mechanochemistry*, in *High Pressure Surface Science and Engineering*, edited by Y. Gogotsi and V. Domnich (Institute of Physics, Bristol, 2004), pp. 159–292.

⁹V. I. Levitas, *Phys. Rev. Lett.* **95**, 075701 (2005).